Crystal structure and X-ray powder diffraction data for two solid-state forms of topiroxostat

Dier Shi, Jiyong Liu, and Xiurong Hu [a)]
Department of Chemistry, Zhejiang University, Hangzhou 310027, PR China

(Received 23 February 2022; accepted 1 August 2022)

X-ray powder diffraction data, unit-cell parameters, and space group for the topiroxostat form II, $C_{13}H_8N_6$, are reported [$a = 7.344(9)$ Å, $b = 12.946(7)$ Å, $c = 12.133(5)$ Å, $\beta = 96.99(3)°$, $V = 1145.2(4)$ Å^3, $Z = 4$, and space group $P2_1/c$]. The topiroxostat monohydrate, $C_{13}H_8N_6 \cdot H_2O$, crystallized in a triclinic system and unit-cell parameters are also reported [$a = 7.422(9)$ Å, $b = 8.552(1)$ Å, $c = 11.193(5)$ Å, $\alpha = 74.85(1)°$, $\beta = 81.17(1)°$, $\gamma = 66.29(1)°$, $V = 627.0(6)$ Å^3, $Z = 2$, and space group P-1]. In each case, all measured lines were indexed and are consistent with the corresponding space group. The single-crystal data of two solid-state forms of topiroxostat are also reported, respectively [$a = 7.346(2)$ Å, $b = 12.955(2)$ Å, $c = 12.130(7)$ Å, $\beta = 96.91(6)°$, $V = 1146.1(3)$ Å^3, $Z = 4$, and space group $P2_1/c$] and [$a = 7.418(6)$ Å, $b = 8.532(8)$ Å, $c = 11.183(9)$ Å, $\alpha = 74.807(1)°$, $\beta = 81.13(1)°$, $\gamma = 66.32(1)°$, $V = 624.7(6)$ Å^3, $Z = 2$, and space group P-1]. The experimental powder diffraction pattern has been well matched with the simulated pattern derived from the single-crystal data. [doi:10.1017/S088571562200029X]

Key words: X-ray powder diffraction data, topiroxostat, solid-state form

I. INTRODUCTION

Topiroxostat (4-(5-(pyridine-4-yl)-1H-1,2,4-triazole-3-yl)pyridine-2-carbonitrile) is a selective xanthine oxidoreductase inhibitor, which is effective in decreasing urinary albumin excretion and reducing the level of serum urate in the human body (Hosoya *et al.*, 2014). Thus, topiroxostat (TOPI) was approved in Japan in June 2013 for the treatment of gout and hyperuricemia (Hosoya *et al.*, 2016). The chemical structure of topiroxostat is shown in Figure 1. As is known that more than half of the pharmaceutical compounds exhibit solid-state polymorphism, and is of great importance as different crystal forms of the drug can show different stability, solubility, dissolution rate and bioavailability, especially for poorly soluble drugs. TOPI has been reported that there are five different crystal forms, such as form I, form II, form III, monohydrate and form A (Lee *et al.*, 2011; Iwabuchi *et al.*, 2014), but their crystal structures have not been reported yet.

We have inspected the Cambridge Structural Database (Groom *et al.*, 2016) and the PDF4 + database (Gates-Rector and Blanton, 2019) and have not found any entries for the topiroxostat form II (TOPI-II) and the topiroxostat monohydrate (TOPI-H_2O) in the mentioned databases. Therefore, we have decided to characterize these compounds by X-ray powder diffraction and X-ray single-crystal diffraction techniques.

II. EXPERIMENTAL

A. Sample preparations

The sample was supplied by Zhejiang Jingxin Pharmaceutical Co., Ltd (purity >99.9%) and used without further purification. Dissolving topiroxostat (400 mg) in anhydrous ethanol (250 ml) and ethanol–water (300 ml, 9:1 v/v), respectively, at reflux temperature and slow cooling of the solutions yielded crystals of TOPI-II and TOPI-H_2O. Then, the crystals were dried, smashed and mounted on a flat zero-background plate.

B. Powder diffraction data collection

X-ray powder diffraction data were collected at room temperature with a SmartLab diffractometer with parafocusing Bragg-Brentano geometry using a Cu Kα radiation (λ = 1.5418 Å) and operated at 40 kV and 180 mA. The D/tex Ultra 250 detector was employed to collect XRD data over

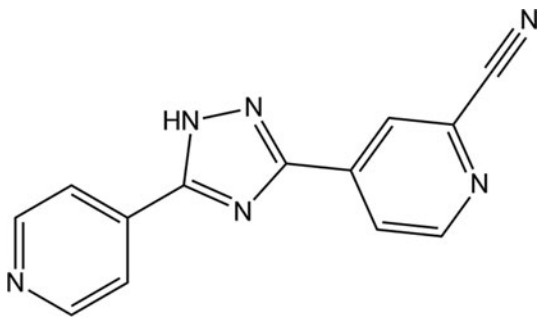

Figure 1. Chemical structure of 4-(5-(pyridine-4-yl)-1H-1,2,4-triazole-3-yl) pyridine-2-carbonitrile.

[a)]Author to whom correspondence should be addressed. Electronic mail: huxiurong@zju.edu.cn

TABLE I. X-ray powder diffraction data of TOPI-II.

$2\theta_{obs}$ (°)	d_{obs} (Å)	$(I/I_o)_{obs}$	h	k	l	$2\theta_{cal}$ (°)	d_{cal} (Å)	$(I/I_o)_{cal}$	$\Delta 2\theta$ (°)
10.018	8.8222	41.9	0	1	1	10.023	8.8180	33	0.005
12.138	7.2858	0.2	1	0	0	12.130	7.2903	0.6	−0.008
13.662	6.4762	7	0	2	0	13.668	6.4734	17.2	0.006
13.922	6.3557	5.6	1	1	0	13.929	6.3524	9.6	0.007
14.698	6.0217	0.4	0	0	2	14.699	6.0217	0.6	0.000
15.047	5.8829	0.3	−1	1	1	15.049	5.8821	0.4	0.002
15.522	5.7039	5.9	0	2	1	15.528	5.7019	11.7	0.005
16.221	5.4598	0.8	0	1	2	16.220	5.4600	3.6	0.000
16.441	5.3872	5	1	1	1	16.439	5.3878	17.4	−0.002
18.319	4.8390	9.5	1	2	0	18.313	4.8405	26.3	−0.006
19.181	4.6233	1.7	−1	2	1	19.185	4.6225	3.8	0.003
20.302	4.3705	12	1	2	1	20.301	4.3707	27.8	−0.001
21.380	4.1526	1.9	1	1	2	21.364	4.1556	6.6	−0.016
21.857	4.0630	0.8	0	3	1	21.859	4.0626	3.1	0.002
22.601	3.9308	7.1	−1	2	2	22.600	3.9311	22.6	−0.001
23.165	3.8365	0.4	0	1	3	23.178	3.8343	1	0.013
23.943	3.7136	0.6	1	3	0	23.942	3.7137	3.3	−0.001
24.939	3.5674	0.6	−1	1	3	24.929	3.5689	1.7	−0.010
25.580	3.4794	4	−2	1	1	25.576	3.4800	8.1	−0.004
26.979	3.3021	100	−2	0	2	26.984	3.3015	100	0.005
27.679	3.2202	13.2	−1	2	3	27.675	3.2206	13.8	−0.004
27.873	3.1982	6.3	−2	1	2	27.865	3.1991	5.1	−0.008
28.268	3.1544	0.2	−2	2	1	28.264	3.1548	2.9	−0.004
28.984	3.0781	0.6	1	3	2	28.997	3.0768	1.8	0.012
30.381	2.9397	1.5	0	3	3	30.385	2.9393	3.3	0.003
30.738	2.9064	0.4	−1	4	1	30.738	2.9064	0.9	0
31.481	2.8394	0.5	−1	1	4	31.477	2.8398	1.7	−0.005
32.303	2.7690	0.1	−2	3	1	32.288	2.7703	1.7	−0.015
32.778	2.7300	0.4	0	2	4	32.778	2.7300	0.9	0.000
33.225	2.6942	−0.1	2	2	2	33.229	2.6939	1	0.004
34.255	2.6156	0.2	1	1	4	34.25	2.616	0.8	−0.005
35.593	2.5202	0.5	0	4	3	35.601	2.5197	0.8	0.008
36.359	2.4689	0.5	1	2	4	36.362	2.4687	1.7	0.003
36.806	2.4399	0.2	1	5	0	36.805	2.4400	0.8	0.002
37.520	2.3951	0.9	−2	3	3	37.525	2.3948	1.7	0.005
37.960	2.3683	0.7	0	1	5	37.965	2.3680	1.6	0.005
38.657	2.3273	0.8	1	4	3	38.658	2.3272	1.1	0.001
39.423	2.2838	0.6	−3	2	1	39.427	2.2835	1.5	0.005
40.893	2.2050	0.5	0	4	4	40.903	2.2045	0.7	0.010
41.442	2.1771	0.7	1	1	5	41.444	2.1769	1	0.002
44.183	2.0482	0.4	1	5	3	44.178	2.0484	0.9	0.004
44.564	2.0315	0.6	0	6	2	44.569	2.0313	3.3	0.005
47.220	1.9232	0.4	−3	2	4	47.209	1.9237	1.4	0.008
49.038	1.8561	0.6	−2	0	6	49.031	1.8564	2.5	0.003

the 2θ range from 3° to 50° with a step size of 0.02° and a counting time of 1.2 s step^{-1}. The software package MDI-Jade version 7.5 (Materials Data Inc., USA) was used to smooth the data, fit the background, strip off the Kα_2 component and obtain the peak positions and intensities (Tables I and II). The K$\alpha_1$was used in converting observed 2θ to d-spacing.

C. Single-crystal diffraction data collection

X-ray single-crystal diffraction data were collected at room temperature with a Bruker D8 Venture diffractometer with Mo Kα radiation ($\lambda = 0.71073$ Å) for cell determination and subsequent data collection. Data reduction was performed by APEX3 software and multi-scan absorption correction was applied. Using Olex2 (Dolomanov *et al.*, 2009), the structures were solved with the ShelXT (Sheldrick, 2015a) structure solution program using intrinsic-phasing and refined with the ShelXL (Sheldrick, 2015b) refinement package using Least Squares minimization.

III. RESULTS AND DISCUSSION

Indexing of the experimental X-ray diffraction patterns and unit-cell refinements were done using MDI-Jade (Materials Data Inc., 2002). The cell refinement results confirmed that TOPI-II is monoclinic with the space group $P2_1/c$ and unit-cell parameters: $a = 7.344(9)$ Å, $b = 12.946(7)$ Å, $c = 12.133(5)$ Å, $\beta = 96.99(3)°$, unit-cell volume $V = 1145.2(4)$ Å^3, $Z = 4$. The figure of merit is $F_{30} = 184.8(0.0053,30)$ (Smith and Snyder, 1979). TOPI-H_2O is also triclinic with the space group P-1 and unit-cell parameters: $a = 7.422(9)$ Å, $b = 8.552(1)$ Å, $c = 11.193(5)$ Å, $\alpha = 74.85(1)°$, $\beta = 81.17(1)°$, $\gamma = 66.29(1)°$, unit-cell volume $V = 627.0(6)$ Å^3 and $Z = 2$. The figure of merit is $F_{30} = 72.5$ (0.013,30) (Smith and Snyder, 1979). The values of $2\theta_{obs}$, d_{obs}, I_{obs}, h, k, l, $2\theta_{cal}$,

https://doi.org/10.1017/S088571562200029X Published online by Cambridge University Press

TABLE II. X-ray powder diffraction data of TOPI-H_2O.

$2\theta_{obs}$ (°)	d_{obs} (Å)	$(I/I_o)_{obs}$	h	k	l	$2\theta_{cal}$ (°)	d_{cal} (Å)	$(I/I_o)_{cal}$	$\Delta 2\theta$ (°)
8.171	10.8124	5.7	0	0	1	8.189	10.7884	12.9	0.018
11.559	7.6495	9.6	0	1	0	11.577	7.6374	20.8	0.018
13.000	6.8044	3.1	1	0	0	13.035	6.7862	4.4	0.035
14.222	6.2227	0.7	1	1	1	14.257	6.2073	4.9	0.035
14.999	5.9018	100	1	0	1	15.025	5.8916	100	0.026
15.601	5.6756	0.1	0	−1	1	15.612	5.6713	0.8	0.012
16.400	5.4006	18.6	0	0	2	16.42	5.3942	26.9	0.02
17.639	5.0241	0.8	−1	−1	1	17.648	5.0216	1.8	0.009
18.759	4.7265	5.7	1	1	2	18.783	4.7205	7	0.024
20.480	4.333	19.5	1	0	2	20.446	4.3401	16.3	−0.034
21.244	4.1789	1.6	1	2	1	21.267	4.1744	3.2	0.023
21.420	4.1449	7.8	−1	1	1	21.426	4.1438	3.2	0.006
21.570	4.1166	1.9	−1	0	2	21.582	4.1143	4.8	0.012
21.940	4.0479	16	1	2	0	21.935	4.0489	25.6	−0.005
22.900	3.8803	0.3	0	2	1	22.908	3.8791	0.7	0.007
23.273	3.8189	0.1	0	2	0	23.275	3.8187	0.4	0.002
23.682	3.754	1.8	1	2	2	23.681	3.7541	2.4	−0.001
23.900	3.7202	3.6	−1	−1	2	23.905	3.7195	5.3	0.005
24.300	3.6599	2.9	2	1	0	24.309	3.6585	6.4	0.009
24.722	3.5984	3	0	0	3	24.737	3.5961	5.6	0.016
25.460	3.4957	28.4	−1	−2	1	25.454	3.4964	47	−0.005
26.999	3.2998	19.8	2	2	1	26.985	3.3015	43.7	−0.015
27.740	3.2133	50.6	2	2	0	27.741	3.2132	98.3	0.001
28.739	3.1038	4	2	2	2	28.741	3.1036	10.2	0.001
29.701	3.0055	0.1	0	−1	3	29.677	3.0078	0.2	−0.024
30.301	2.9474	1.6	2	0	2	30.317	2.9458	3	0.016
30.841	2.8969	4.5	−2	−2	1	30.84	2.897	9.2	−0.001
31.357	2.8505	0.8	1	3	1	31.361	2.8501	5	0.004
31.500	2.8378	3.1	0	−2	2	31.525	2.8357	5	0.024
32.659	2.7397	3.7	0	1	4	32.655	2.74	5.2	−0.005
33.200	2.6963	4.5	0	0	4	33.19	2.6971	5.2	−0.01
33.461	2.6759	0.1	−2	1	1	33.444	2.6772	2.9	−0.017
34.039	2.6317	0.4	2	−1	1	34.022	2.633	0.7	−0.017
35.227	2.5456	0.5	0	3	0	35.225	2.5458	0.9	−0.002
35.481	2.528	1	0	3	2	35.488	2.5275	1.4	0.007
36.261	2.4754	1.5	0	2	4	36.262	2.4753	2.5	0
36.941	2.4314	0.7	−1	2	3	36.953	2.4306	1.3	0.012
38.040	2.3636	2.5	0	−3	1	38.035	2.3639	2.3	−0.005
38.541	2.334	1.6	0	3	3	38.526	2.3349	3.3	−0.015
40.800	2.2099	3	1	1	5	40.798	2.21	3.7	−0.002
41.601	2.1692	6.9	2	0	4	41.583	2.1701	3.7	−0.018
41.820	2.1583	3	1	2	5	41.829	2.1578	4.1	0.009
42.400	2.1301	0.3	−1	2	4	42.38	2.1311	1	−0.02
42.920	2.1055	0.7	−2	−3	2	42.939	2.1046	1.7	0.019
44.721	2.0248	1.2	−1	0	5	44.728	2.0245	2	0.008
45.216	2.0038	0.1	−1	1	5	45.211	2.004	1	−0.005
45.695	1.9838	0.7	−1	3	3	45.646	1.9859	0.4	−0.049
46.660	1.9451	1.3	−3	1	1	46.652	1.9454	1.8	−0.008
48.462	1.8769	0.5	2	4	4	48.456	1.8771	1.2	−0.005
48.899	1.8611	0.7	0	3	5	48.905	1.8609	1.5	0.005
49.420	1.8427	2.3	0	1	6	49.404	1.8433	4.4	−0.016

d_{cal}, I_{cal} and $\Delta 2\theta$ are listed in Tables I and II. Because the morphology of TOPI-II and TOPI-H_2O was plate crystals with preferred orientations, there is a minor difference in the relative intensities of the diffraction peaks between the experimental X-ray diffraction patterns and the calculated XRD patterns.

Based on the single-crystal data, the structures of TOPI-II and TOPI-H_2O were solved and refined. The detailed crystallographic information is summarized in Supplementary Tables SI–SIII, and the asymmetric units of both forms with the corresponding atom labeling scheme are illustrated in Figure 2. In the crystal structure of TOPI-II, there is one topiroxostat molecule in the asymmetric unit, which is connected by hydrogen bond N2–H4···N6^{i} [symmetric code: (i) $2-x$, $1/2+y$, $3/2-z$] to form an infinite "zigzag" chain along the b-axis. The asymmetric unit of TOPI-H_2O contains a topiroxostat molecule and an H_2O molecule. In the crystal structure, the H_2O molecule was involved in hydrogen bonding (O1–H1B···N2^{ii}, O1–H1A···N6^{iii}, N4–H4···O1, [symmetric code: (ii) x, y, $-1+z$; (iii) $-1+x$, $1+y$, z]) with the topiroxostat molecule forming hydrogen two-dimensional hydrogen-bond networks.

In addition, there are good agreements between the experimental powder diffraction pattern and the simulated pattern

https://doi.org/10.1017/S088571562200029X Published online by Cambridge University Press

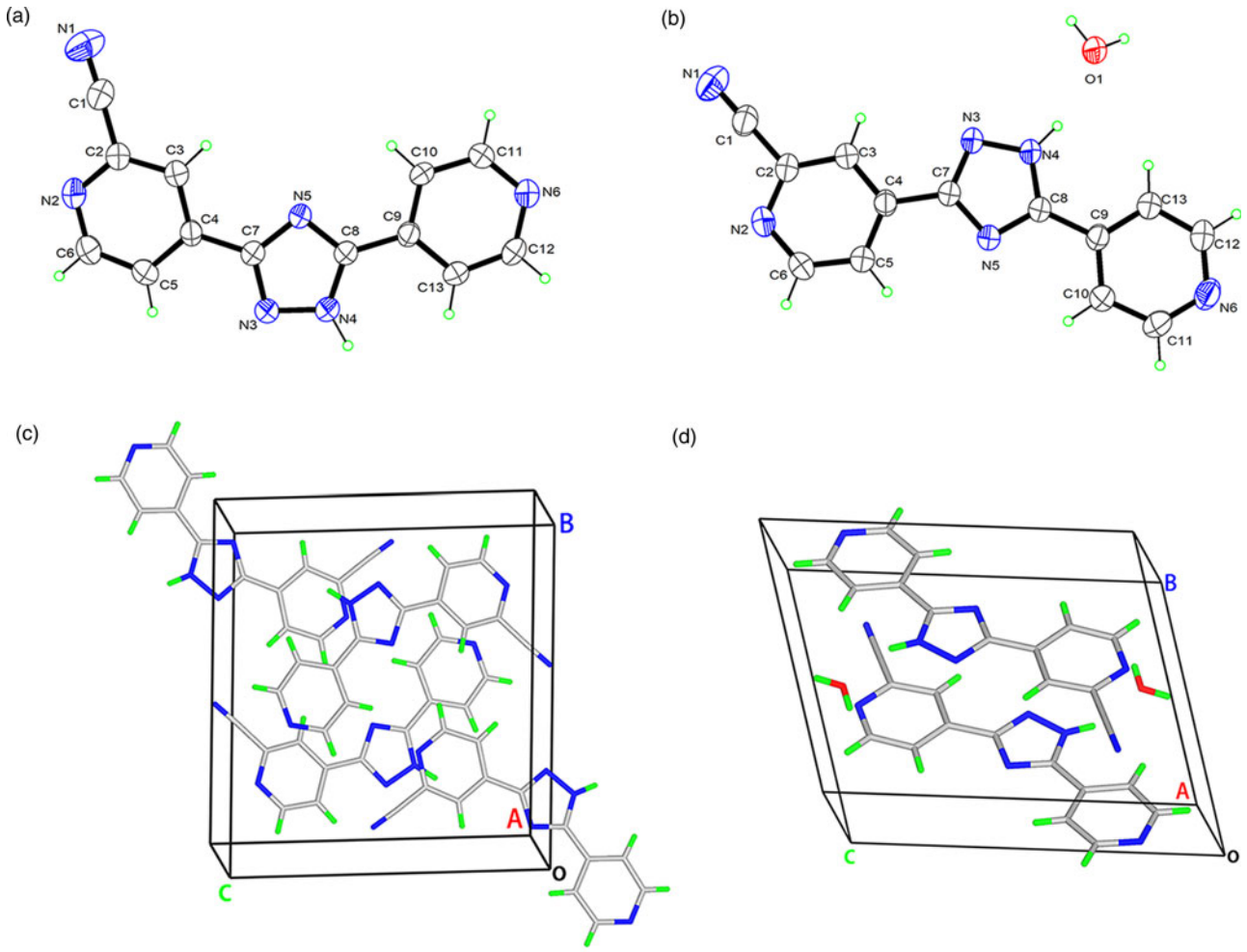

Figure 2. Asymmetric unit of TOPI-II (a) and TOPI-H_2O (b) shown in the thermal ellipsoid model with 50% probability. The crystal packing of TOPI-II (c) and TOPI-H_2O (d) in the unit cell.

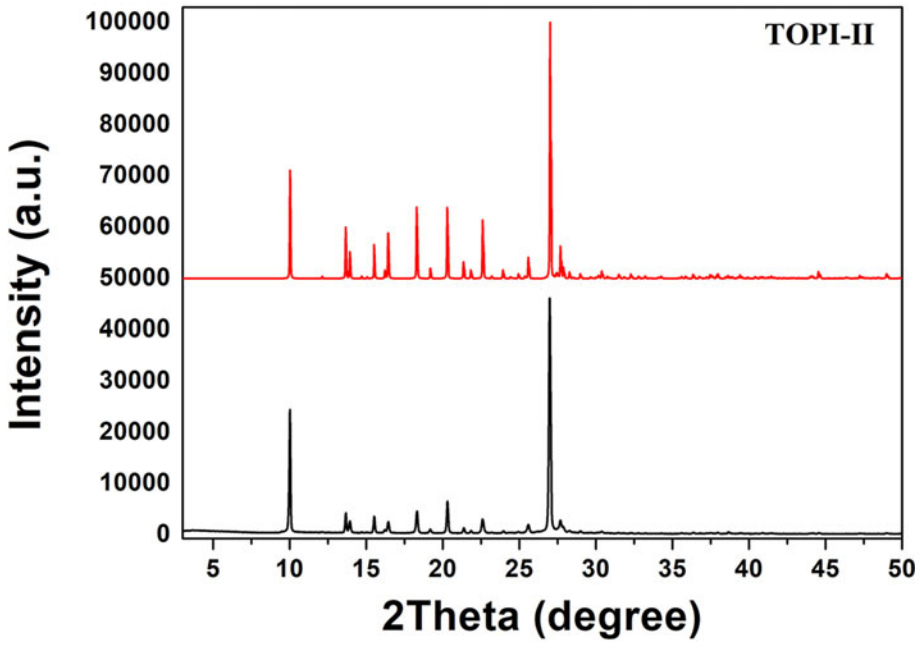

Figure 3. X-ray powder diffraction pattern (black line) and the simulated pattern of the crystal structure (red line) of TOPI-II.

https://doi.org/10.1017/S088571562200029X Published online by Cambridge University Press

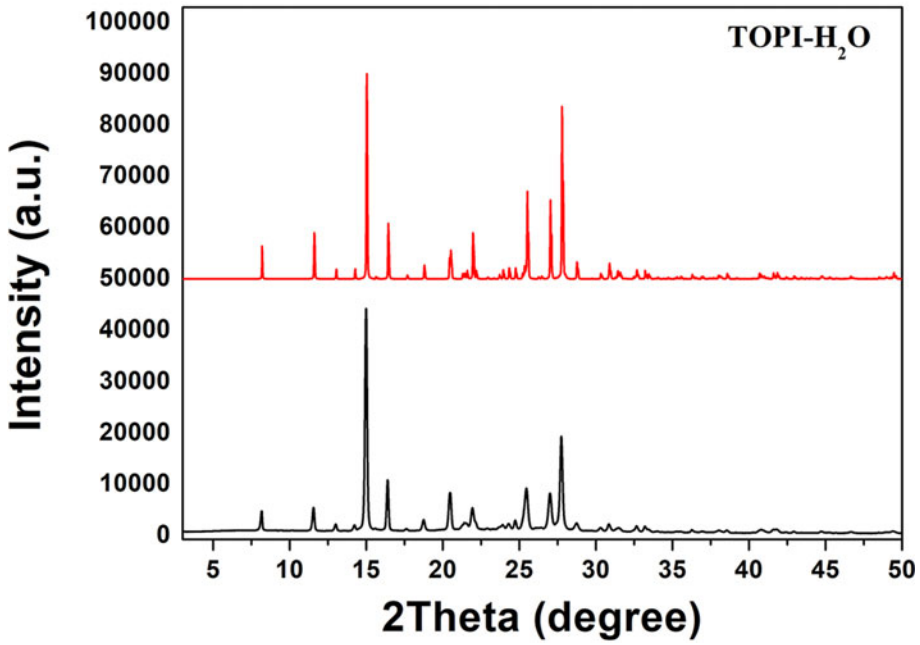

Figure 4. X-ray powder diffraction pattern (black line) and the simulated pattern of the crystal structure (red line) of TOPI-H_2O.

derived from the single-crystal data (Figures 3 and 4). The deviations of the unit-cell parameters and unit-cell volume of TOPI-II were between 0.07% and 0.08%. The deviations of the unit-cell parameters and unit-cell volume of TOPI-H_2O were between 0.23% and 0.37%.

SUPPLEMENTARY MATERIAL

The supplementary material for this article can be found at https://doi.org/10.1017/S088571562200029X.

FUNDING INFORMATION

This work was financially supported from Zhejiang University Experimental Technology Research (SYB202103).

Dolomanov, O. V., Bourhis, L. J., Gildea, R. J., Howard, J. A. K., and Puschmann, H. (**2009**). "OLEX2: a complete structure solution, refinement and analysis program," J. Appl. Crystallogr. **42**, 339–341.

Gates-Rector, S. and Blanton, T. (**2019**). "The powder diffraction file: a quality materials characterization database," Powd. Diffr. **34**, 352–360.

Groom, C. R., Bruno, I. J., Lightfoot, M. P., and Ward, S. C. (**2016**). "The Cambridge structural database," Acta Crystallogr. **72**, 171–179.

Hosoya, T., Ohno, I., Nomura, S., Hisatome, I., Uchida, S., Fujimori, S., Yamamoto, T., and Hara, S. (**2014**). "Effects of topiroxostat on the serum urate levels and urinary albumin excretion in hyperuricemic stage 3 chronic kidney disease patients with or without gout," Clin. Exp. Nephrol. **18**, 876–884.

Hosoya, T., Sasaki, T., Hashimoto, H., Sakamoto, R., and Ohashi, T. (**2016**). "Clinical efficacy and safety of topiroxostat in Japanese male hyperuricemic patients with or without gout: an exploratory, phase 2a, multicentre, randomized, double-blind, placebo-controlled study," J. Clin. Phar. Ther. **41**, 298–305.

Iwabuchi, Y., Miyata, S., Sato, T., Uda, J., Kandou, T., Inoue, T., and Nakano, H. (**2014**). "4-(5-(pyridine-4-yl)-1H-1,2,4-triazole-3-yl)pyridine-2-carbonitrile crystalline polymorph and production method therefor," the Patent Corporate Body Aruga Patent Office WO2014017515A.

Lee, A. Y., Erdemir, D., and Myerson, A. S. (**2011**). "Crystal polymorphism in chemical process development," Annu. Rev. Chem. Biomol. Eng. **2**, 259–280.

Materials Data Inc. (MDI) and the International Centre for Diffraction Data (ICDD). (**2002**). Jade 7.5 XRD Pattern Processing Software.

Sheldrick, G. M. (**2015a**). "SHELXT - integrated space-group and crystal-structure determination," Acta Crystallogr. **A71**, 3–8.

Sheldrick, G. M. (**2015b**). "Crystal structure refinement with SHELXL," Acta Crystallogr. **C71**, 3–8.

Smith, G. S. and Snyder, R. L. (**1979**). "F_N: a criterion for rating powder diffraction patterns and evaluating the reliability of powder-pattern indexing," J. Appl. Crystallogr. **12**, 60–65.